
Volume 300, Issues 3–4
1 December 2010
ISSN 0012-821X
ELSEVIER
EARTH
& PLANETARY
SCIENCE LETTERS
Editors
Rick Carlson, Washington, DC
Peter B. deMenocal, Palisades, NY
T. Mark Harrison, Los Angeles, CA
Yanick Ricard, Lyon
P. Shearer, La Jolla, CA
Tilman Spohn, Berlin
Lars Stixrude, London

Earth and Planetary Science Letters 300 (2010) 329–342

Contents lists available at ScienceDirect

Earth and Planetary Science Letters

journal homepage: www.elsevier.com/locate/epsl

North Atlantic climate evolution through the Plio-Pleistocene climate transitions

K.T. Lawrence [a,*], S. Sosdian [b,c], H.E. White [a], Y. Rosenthal [c]

[a] Lafayette College, Department of Geology and Environmental Geosciences, 102 Van Wickle Hall, Easton, PA 18042, USA
[b] School of Earth and Ocean Sciences, Cardiff University, Main Building, Park Place, Cardiff, CF10 3YE, Wales, United Kingdom
[c] Institute of Marine and Coastal Sciences and Department of Earth and Planetary Sciences, Rutgers University, New Brunswick, NJ 08901, USA

ARTICLE INFO

Article history:
Received 6 July 2010
Received in revised form 28 September 2010
Accepted 11 October 2010
Available online 17 November 2010

Editor: P. DeMenocal

Keywords:
North Atlantic
Pliocene
Pleistocene
sea surface temperature
bottom water temperature
alkenones

ABSTRACT

During the Plio-Pleistocene, the Earth witnessed the growth of large northern hemisphere ice sheets and profound changes in both North Atlantic and global climate. Here, we present a ~3.2 Myr long, orbitally-resolved alkenone sea surface temperature (SST) record from Deep Sea Drilling Project (DSDP) Site 607 (41°N, 33°W, water depth 3427 m) in the North Atlantic Ocean. We employ a multi-proxy approach comparing these new observations with existing bottom water temperature (BWT) and stable isotope time series from the same site and SST time series from other sites, shedding new light on Plio-Pleistocene climate change. North Atlantic temperature records show a long-term cooling with two major steps occurring during the late Pliocene (3.1 to 2.4 Ma) and the mid-Pleistocene (1.5 to 0.8 Ma), closely timed with intervals of major change in northern hemisphere ice sheets. Existing evidence suggests that the late Pliocene cooling may have been caused by a thresholded response to secular changes in atmospheric carbon dioxide (CO_2). While an explanation for the mid-Pleistocene cooling may involve glacial–interglacial changes in atmospheric CO_2, it seems to also require a change in the behavior of the ice sheets themselves. North Atlantic climate responses were closely phased with benthic oxygen isotope ($\delta^{18}O$) changes during the "41 kyr world," indicating a strong common northern hemisphere high latitude imprint on North Atlantic climate signals. After the mid-Pleistocene transition (MPT), North Atlantic SST records and the Site 607 benthic carbon isotope ($\delta^{13}C$) record are more closely phased with $\delta^{18}O$, whereas BWT significantly leads $\delta^{18}O$ in the 100 kyr band, suggesting a shift from a northern to a southern hemisphere influence on North Atlantic BWT. We propose that the expansion of the West Antarctic ice sheet (WAIS) across the MPT increased the production and export of Antarctic Bottom Water from the Southern Ocean and subsequently controlled its incursion into the North Atlantic, especially during glacial intervals. It follows that the early 100 kyr response of BWT implies an early response of the WAIS relative to the northern hemisphere deglaciation. Thus, in the "100 kyr world," both northern hemisphere and southern hemisphere processes affect climate conditions in the North Atlantic Ocean.

1. Introduction

1.1. Plio-Pleistocene climate change

Over the past 5 million years the Earth's climate system underwent two major transitions. The first transition, which occurred in the late Pliocene (referred to hereafter as the late Pliocene transition (LPT)) was marked by a shift from largely ice-free conditions in the northern hemisphere (NH) to extensive NH continental glaciation (Ravelo et al., 2004, 2007; Raymo, 1994). The second transition, which occurred during the mid-Pleistocene and is referred to as the mid-Pleistocene transition (MPT), witnessed a fundamental shift in the periodicity of climate cycles from glacial–interglacial beats occurring every 41 thousand years to those occurring every 100 thousand years as well as a growth in the variance and asymmetry associated with these glacial–interglacial oscillations (Clark et al., 2006; de Garidel-Thoron et al., 2005; Imbrie et al., 1993; Lisiecki and Raymo, 2007; Liu and Herbert, 2004; Pisias and Moore, 1981; Shackleton and Opdyke, 1976). While evidence of these transitions is found in climate records from around the world, the North Atlantic Ocean, due to its location most proximal to growing NH ice sheets, was not only the region most significantly impacted by changes during these climate transitions, but has also been cited as playing a leading role in driving the ice age cycles themselves (Imbrie et al., 1992, 1993).

1.2. Secular changes in Plio-Pleistocene climate

Determining the cause(s) of the Plio-Pleistocene climate transitions has been a focus of paleoclimate research for decades. Two main mechanisms, altered heat transport and elevated atmospheric CO_2 (pCO_2), have persisted as potential candidates for explaining the shift

* Corresponding author. Tel.: +1 610 330 5194; fax: +1 610 330 5717.
E-mail addresses: lawrenck@lafayette.edu (K.T. Lawrence), sosdian@imcs.rutgers.edu (S. Sosdian), hwhite962@gmail.com (H.E. White), rosentha@marine.rutgers.edu (Y. Rosenthal).

0012-821X/$ – see front matter © 2010 Elsevier B.V. All rights reserved.
doi:10.1016/j.epsl.2010.10.013

from the nearly ice-free conditions that existed during the early Pliocene warm period (3–5 Ma), to the more glaciated conditions that developed during the late Pliocene and Pleistocene and remain a feature of the modern NH climate system. The closure of two low latitude ocean gateways, the Panamanian Seaway and the Indonesian Throughflow, have figured prominently in arguments for altered heat transport as the explanation for the end of the early Pliocene warm period (Cane and Molnar, 2001; Driscoll and Haug, 1998; Haug and Tiedemann, 1998; Steph et al., 2010). These hypotheses tie long-term tectonic movements to changes in atmospheric and/or ocean circulation that influenced heat transport to high northern latitudes. Another set of arguments for the LPT focus on long-term changes in the composition of the atmosphere and the influence of these changes on the development of significant glaciation in the NH (DeConto et al., 2008; Lunt et al., 2008; Seki et al., 2010). While all methodologies for estimating past pCO_2 are hampered by considerable uncertainties, numerous studies from a disparate set of methodologies seem to converge on the same broad conclusion that atmospheric CO_2 during the early Pliocene was around 330–415 ppm, modestly higher than pre-industrial values (Kürschner et al., 1996; Pagani et al., 2009; Raymo et al., 1996; Seki et al., 2010; Tripati et al., 2009; Van Der Burgh et al., 1993). Which of these two classes of mechanisms account for the LPT or whether or not both figure prominently in this climate story remains an open question.

The cause of the frequency and amplitude shifts that occurred during the MPT is perhaps even more enigmatic. The shift in the primary beat of glacial–interglacial cycles from 41 kyr to 100 kyr periodicity is unaccompanied by a corresponding change in orbital forcing, indicating that a change in orbital variations cannot be the primary explanation for this frequency shift (Berger et al., 1999). Furthermore, although the 100 kyr periodicity of late Pleistocene glacial cycles is consistent with the tempo of variations in orbital eccentricity, changes in solar radiation driven by eccentricity are far too small to account for the large amplitude fluctuations in climate observed in the geologic record (Imbrie et al., 1992, 1993). Proposed explanations for the MPT fall into two categories: a non-linear climate system response to a long-term cooling (Berger et al., 1999; Paillard, 1998; Raymo, 1997; Rial, 2004), or a transition within the climate system related to the thickness and instability of ice sheets (Clark et al., 2006; Clark and Pollard, 1998; Raymo et al., 2006). The first group of explanations attributes the MPT to a global cooling, possibly caused by a secular decrease in greenhouse gases, specifically pCO_2 (Berger et al., 1999; Paillard, 1998; Raymo, 1997; Rial, 2004). These "cooling hypotheses" suggest that a colder climate enables the growth of larger ice sheets and the rise of the 100 kyr cycle, because large ice sheets are capable of surviving through moderate insolation maxima, deglaciating only under more rarely occurring pronounced maxima in insolation forcing. In contrast, the "regolith hypothesis" of Clark and Pollard (1998) argues that the size of northern hemisphere ice sheets during the early Pleistocene was constrained by the occurrence of an unstable regolith substrate which led to laterally extensive but thin ice sheets. According to Clark and Pollard (1998), the exposure of the high friction substrate of Precambrian Shield bedrock by repeated glacial erosion allowed for the buildup of thicker ice sheets, which gave rise to 100 kyr glacial cycles during the late Pleistocene. Thus far, no hypothesis put forth to explain the MPT has been able to satisfactorily account for all of the existing paleoclimate observations.

1.3. Orbital scale changes in Plio-Pleistocene Climate

Classic Milankovitch Theory and the seminal SPECMAP Project (Imbrie et al., 1992, 1993) also implicate North Atlantic climate processes as pivotal to the series of climate system responses that unfolded on glacial–interglacial timescales. The SPECMAP Project examined the relative phasing of existing late Pleistocene climate system responses derived from a set of geographically diverse localities. Their analysis suggested that the sequence of climate system responses in all three orbital bands (i.e. 100 kyr, 41 kyr, and 23 kyr) was the same and that these responses could be broadly divided into "early" and "late" response groups which were respectively controlled by fast responding (e.g. ocean circulation, sea ice, and ocean chemistry) versus slow responding (i.e. ice sheet buildup or melting) components of the climate system. Based upon these phase relationships and classic Milankovitch Theory, which posits that NH summer insolation is the driver of glacial–interglacial variations in climate, SPECMAP proposed a conceptual model of the progression of climate system responses through glacial–interglacial cycles during the late Pleistocene triggered by an event in the Nordic Seas. According to the SPECMAP framework, North Atlantic climate responses consistently fall into the group of late responders, implying moderation by NH ice sheets.

In this study, we offer new insight into the Plio-Pleistocene climate history of the North Atlantic Ocean. Using a multi-proxy approach, we provide a synthesis of North Atlantic climate evolution over the past 3.2 million years by comparing a new orbitally-resolved, alkenone-derived, SST record to previously published orbital-resolution surface temperature (Lawrence et al., 2009), bottom water temperature (Sosdian and Rosenthal, 2009) and stable isotope datasets (Raymo et al., 1989; Ruddiman et al., 1989) from this region. This analysis enables us to evaluate both the long-term and orbital scale evolution of North Atlantic climate. We find a remarkably consistent response among North Atlantic climate records on both secular and orbital timescales, suggesting a coordinated North Atlantic response to climate change through most of the Plio-Pleistocene. However, phase relationships among North Atlantic climate variables during the late Pleistocene suggest that southern hemisphere climate processes exerted influence on North Atlantic climate conditions on 100 kyr time scales after the mid-Pleistocene transition.

2. Methods

2.1. Site and proxy background

We present a new orbitally-resolved, alkenone-derived SST record from Deep Sea Drilling Project (DSDP) Site 607 (41°N, 33°W, 3427 m, mean annual surface temperature 18.5 °C) (Fig. 1). Site 607 is located on the western flank of the Mid-Atlantic Ridge underlying the northern edge of the North Atlantic subtropical gyre. Sedimentation rates at Site 607 across the interval studied averaged ~4.5 cm/kyr. The novel paleotemperature estimates presented in this study were produced using alkenone paleothermometry. Alkenones are a suite of organic compounds synthesized by a few species of ocean surface dwelling algae (Brassell et al., 1986; Marlowe et al., 1984; Prahl and Wakeham, 1987). The alkenone unsaturation index ($U^{k'}_{37} = [C_{37:2}]/[C_{37:2}] + [C_{37:3}]$) has been linearly calibrated to organism growth temperature and thus has been used as a means of estimating past ocean surface temperatures (Brassell et al., 1986; Prahl and Wakeham, 1987). Here, we used the Prahl et al. (1988) calibration to convert alkenone unsaturation indices into estimates of past SST. Extensive core-top calibration studies indicate the global applicability of this calibration function (Müller et al., 1998). We assume this modern calibration is applicable over the 3.2 Myr time scale examined in this study.

2.2. Alkenone analysis

Alkenones were extracted from freeze-dried sediment samples in a Dionex accelerated solvent extractor (ASE) 200. We extracted alkenones and other lipid compounds from sediment samples that averaged ~3–5 g dry weight. The extraction method entailed three fill, hold, flush, and purge cycles in which sample vessels are filled with

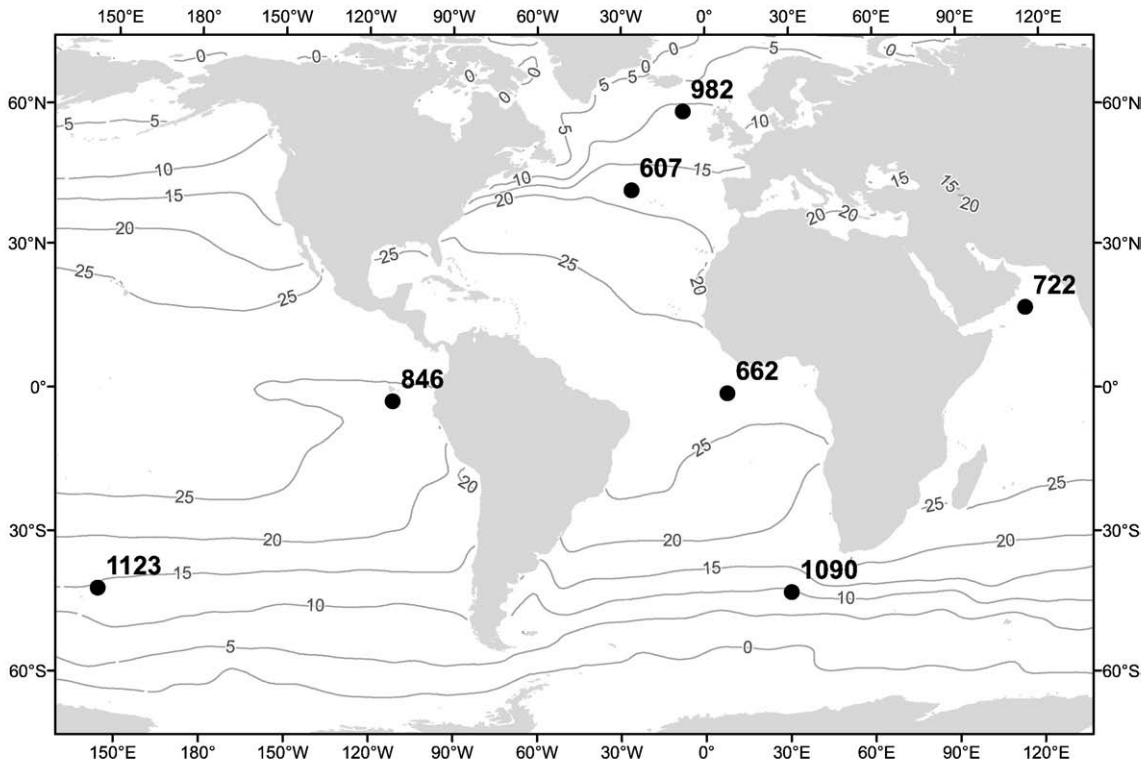

Fig. 1. Site map. Locations of relevant sites superimposed on a map of mean annual SST (Locarnini et al., 2006).

100% dicholoromethane, heated to 150 °C, pressured to 1500 psi, and then flushed into a collection vial. The ~20 to 30 ml of total lipid extract from each sample was then evaporated under a nitrogen stream and reconstituted using 200 µl of toluene, which was previously spiked with n-hexacontracontane (C_{36}) and n-heptatriacontane (C_{37}) standards. We used an Agilent 6890 gas chromatograph (GC) equipped with a flame ionization detector to quantify the concentration of C_{37} alkenones in each of our sediment samples. Depending on the alkenone concentrations in each sample 1–5 µl were injected into an Agilent Technologies DB-1 column (60 m × 0.32 mm × 0.10 µm film thickness). The GC temperature program started from an initial temperature of 90 °C, ramping at an initial rate of 30 °C/min to 260 °C, then ramping slowly at a rate of 1 °C/min to 300 °C, and finishing with a post run temperature of 315 °C for 10 min. Reproducibility based on replicate samples analysis is $\pm 0.007 U^{K'}_{37}$ units, equivalent to ± 0.2 °C using the Prahl et al. (1988) calibration employed here. Alkenone concentrations in Site 607 samples ranged from 11 ng/g to 6560 ng/g. Comparing our alkenone estimates to previously published faunal SST estimates (Ruddiman and McIntyre, 1984; Ruddiman et al., 1989) from Site 607 suggests that alkenone-derived SST estimates at this site are recording mean annual surface temperature, as alkenone SST estimates consistently lie in between the faunal winter and summer SST estimates for the ~1 Myr interval of overlapping data.

2.3. North Atlantic synthesis data analysis

We use our Site 607 SST record in conjunction with previously published bottom water temperature (BWT) (Sosdian and Rosenthal, 2009) and stable isotope records from Site 607 (Raymo et al., 1989; Ruddiman et al., 1989; Raymo et al., 1992) and an SST record from Ocean Drilling Program (ODP) 982 (58°N, 16°W, 1134 m, mean annual surface temperature 11 °C) (Lawrence et al., 2009) located south of Iceland on the Rockall Plateau (Fig. 1) to provide a synthetic view of both secular and orbital scale North Atlantic climate evolution over the past 3.2 Myr. Age models for both ODP Site 982 and DSDP Site 607 were obtained directly from L. Lisiecki, who used both of these datasets in the development of the LR04 stack (Lisiecki and Raymo, 2005). The average sample resolution for all DSDP Site 607 records is 3–4 kyr (Raymo et al., 1989; Ruddiman et al., 1989; Sosdian and Rosenthal, 2009; Raymo et al., 1992). The alkenone SST record from Site 982 is sampled at an average of ~3 kyr resolution for the intervals between 4 to 2.5 Ma, 1.75 to 1.25 Ma, and 0.4 to 0 Ma [Lawrence et al., 2009). The intervening intervals were sampled at ~10 kyr resolution (Lawrence et al., 2009). We used the Arand software package (Howell, 2001) to perform all spectral, phase, and coherency analyses. We present evolutionary spectra both with and without prewhitening in order to explore both high and low frequency Milankovitch periodicity present in our records. Prewhitening helps attenuate the red spectrum background produced by the long-term trend of the records, which allows for better resolution of higher frequency Milankovitch beats (23 kyr and 41 kyr) but also dampens the spectral density in the lower frequency part of the spectrum (i.e. attenuates the 100 kyr power). For clarity, we present coherency comparisons of proxy phase relationships for representative time windows during the "41 kyr world" of the Pliocene (2.7 to 2.2 Ma) as well as the "100 kyr world" of the late Pleistocene (0.75 Ma to 0.25 Ma). Our chosen time windows were dictated by the oldest and youngest overlapping segments of all time series and by time intervals in which all proxies were coherent with the benthic oxygen isotope ($\delta^{18}O_c$) record. Coherency and phase results for adjacent time windows yield coherency and phase results consistent with those reported here.

We interpret the $\delta^{18}O_c$ from Site 607 primarily as a measure of ice volume and the benthic carbon isotope signal ($\delta^{13}C$) as an indicator for deep ocean circulation. DSDP Site 607 in the modern-day is saturated with North Atlantic Deep Water (NADW) (characterized by high $\delta^{13}C$), but during the last glacial maximum, evidence suggests that the influence of Antarctic Bottom Water (AABW) (characterized by low $\delta^{13}C$), a southern source water mass, was significant (Boyle and Keigwin, 1982; Boyle and Keigwin, 1985/86; Oppo and Fairbanks, 1987; Raymo et al., 1997). Variations in $\delta^{13}C$ at this site across the Plio-Pleistocene were interpreted as changes in the relative proportions of

NADW and AABW. We infer that BWT at Site 607, while recorded in the benthic foraminifera at 41°N, must derive its signal from properties of the water column imparted in high latitude, deep water formation regions. We attribute trends and variations in alkenone-derived SST records from Sites 607 and 982 to both global and regional climatic changes.

3. Results

3.1. Secular trends in Plio-Pleistocene climate

North Atlantic SST and BWT records and the Site 607 $\delta^{18}O$ time series indicate a long-term cooling over the past 3.2 Myr (Figs. 2, 3; Table 1). All North Atlantic time series exhibit remarkably consistent structure on both secular and orbital timescales (Figs. 2, 3; S1), providing strong validation for these proxies as measures of past climatic variations. These datasets demonstrate that the Plio-Pleistocene climate shift was marked by two different intervals of long-term cooling. The first interval was manifested by a time transgressive surface ocean cooling evident in the earliest portion of our temperature records. Both 982 SST and 607 BWT synchronously cool ~2 °C between the start of our shortest dataset (607 BWT) at ~3.2 and 2.4 Ma (Figs. 1, 3). Site 607 SST has a longer (~3 to 2 Ma) and larger (~3 °C) cooling step (Figs. 1, 3). Previous work (Lawrence et al., 2009) suggests that this Pliocene cooling interval started before the 3.2 Myr of climate history captured here. The second cooling interval, a 1.5 to 2.5 °C cooling, started in the early Pleistocene between ~1.5 and 1.3 Ma, and ended ~0.95 to 0.8 Ma, the time typically associated with MPT frequency and amplitude shifts in many paleoclimate time series (Figs. 2, 3). Because we used the last data point from a 400 kyr running smoothed mean to calculate the time series of temperature change (Fig. 3), we acknowledge that the absence of data in our Site 607 SST record for the last 250 kyr, which should contain the coldest values of the long-term running smoothed mean, may slightly attenuate the magnitude of temperature change we estimate for this site.

To explore the relative influences of cooling during glacial versus interglacial intervals in driving the long-term evolution of mean temperature, we used glacial and interglacial values named in the LR04 benthic $\delta^{18}O$ stack (Lisiecki and Raymo, 2005) to identify corresponding glacial and interglacial SST and BWT estimates in Site 607 and Site 982 temperature records. These time series of glacial and interglacial extrema reveal differing patterns of cooling during the two observed long-term cooling steps (Fig. 4). During the LPT, glacial and interglacial cooling is of similar magnitude in each record. In

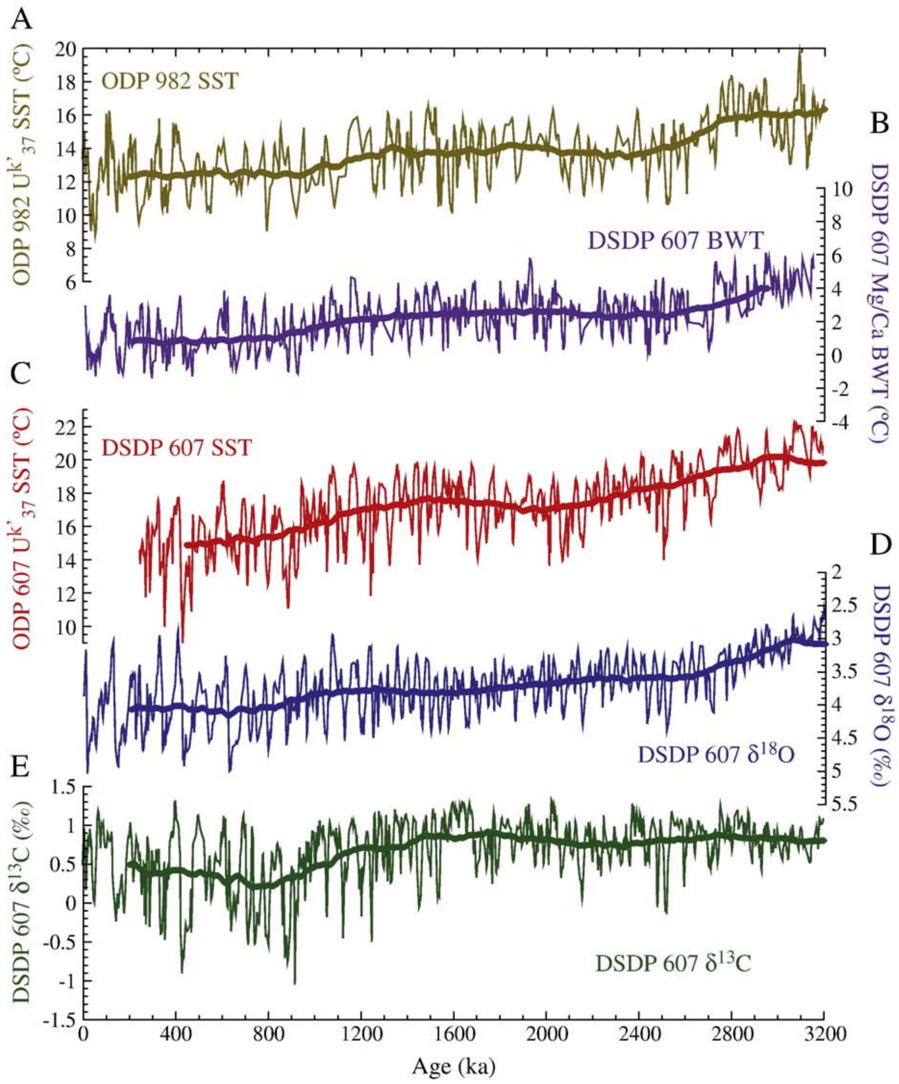

Fig. 2. North Atlantic paleoclimate time series. A) ODP Site 982 $U^{k'}_{37}$ SST (brown line) (Lawrence et al., 2009), B) DSDP Site 607 Mg/Ca BWT (purple line) (Sosdian and Rosenthal, 2009), C) DSDP Site 607 SST (red line), D) DSDP Site 607 $\delta^{18}O_c$ (blue line) (Raymo et al., 1989; Ruddiman et al., 1989; Raymo et al., 1992), E) DSDP Site 607 $\delta^{13}C$ (green line) (Raymo et al., 1989; Ruddiman et al., 1989; Raymo et al., 1992). The thick lines in each time series plot are smoothed running means using a 400 kyr window. Note that y-axes in each temperature plot are scaled to comparable magnitudes.

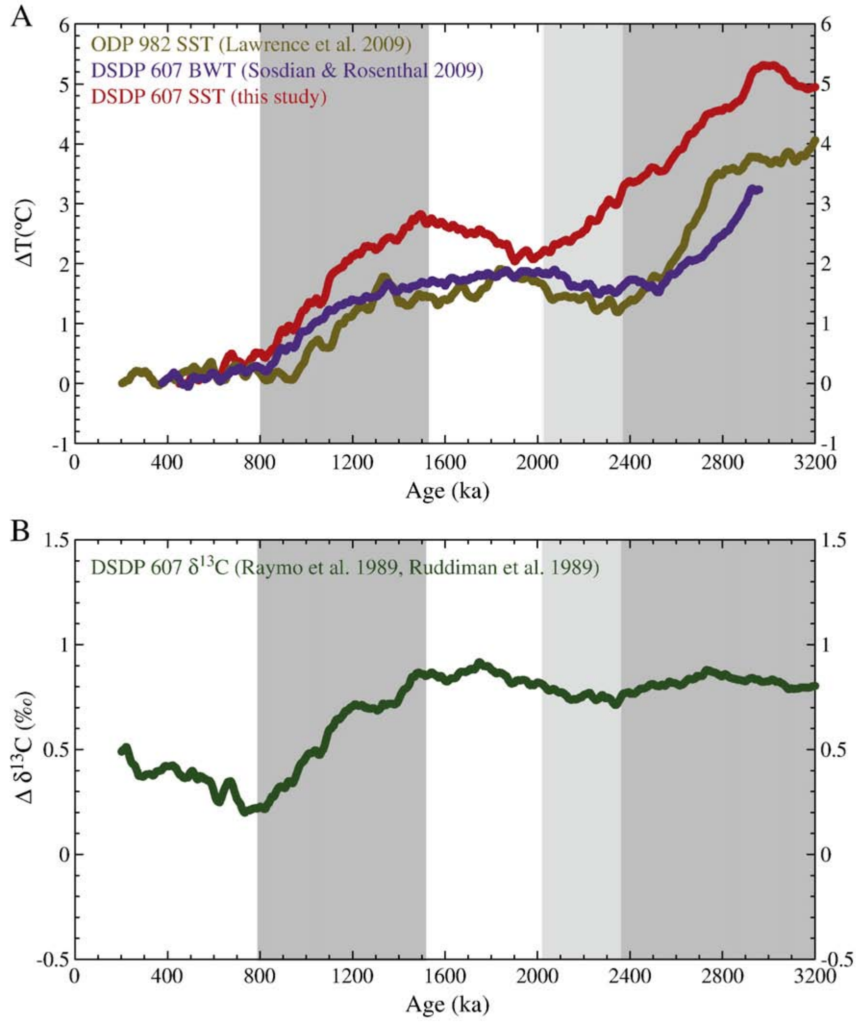

Fig. 3. Secular changes in paleoclimate time series. A) Paleotemperature time series from the North Atlantic: ODP 982 SST (brown line) (Lawrence et al., 2009), DSDP 607 BWT (purple line) (Sosdian and Rosenthal, 2009) and DSDP 607 SST (red line). B) Carbon isotopes from DSDP 607 (green line) (Raymo et al., 1989; Ruddiman et al., 1989; Raymo et al., 1992). We computed the change in temperature by taking a 400 kyr running smoothed mean of each time series and subtracting the most recent value in each smoothed time series from all other data points in the smoothed time series. Note the two intervals of significant cooling (shaded dark gray) across the LPT and before the MPT shared by all three records as well as the extended duration of cooling during the LPT in the 607 SST record indicated by light gray shading.

contrast, during the Pleistocene cooling step (1.5 to 0.8 Ma) the pattern of temperature change between glacials and interglacials is asymmetric. The cooling of glacial intervals is pronounced in all records, whereas there is minimal temperature change during interglacials (Fig. 4).

Table 1
Statistical summary of the primary features of North Atlantic and tropical temperature records from different time intervals.

Time interval (kyr)	0 to 850 ka	1150 to 2500 ka	3000 to 3150 ka
Sites	Mean T (°C)	Mean T (°C)	Mean T (°C)
DSDP 607 BWT[a]	0.8	2.4	4.3
ODP 982 SST[b]	12.5	13.8	15.5
DSDP 607 SST	15.0	17.5	20.4
ODP 846 SST[c]	22.3	23.8	25.6
ODP 662 SST[d]	24.6	25.9	26.8
ODP 722 SST[d]	25.8	26.7	27.1

Data for these estimates were derived from time series published in the following references.
[a] Sosdian and Rosenthal, 2009.
[b] Lawrence et al., 2009.
[c] Lawrence et al., 2006; Liu and Herbert, 2004.
[d] Cleaveland and Herbert, 2007; Herbert et al., 2010.

3.2. Orbital scale patterns during the Plio-Pleistocene

While the 100 kyr cycles of the late Pleistocene account for the most variance in each North Atlantic paleoclimate record, 41 kyr beats strongly modulated by changes in obliquity amplitude dominate variations in all records throughout the Pliocene and early Pleistocene (Figs. 5, 6). All time series exhibit the classic orbital scale frequency shift from dominant 41 kyr beats to dominant 100 kyr beats. The frequency shift starts as a broad band of spectra power in the ~80 to 100 kyr band in the temperature time series at ~1.4 Ma (Fig. 5A,B,C) about synchronous with the start of the Pleistocene cooling step (1.5 to 1.3 Ma) that is evident in these records (Figs. 3, 5). A narrow and persistent 100 kyr signal emerges in all North Atlantic climate records across the MPT, ~1 to 0.75 Ma (Fig. 5). We observe the presence of 100k power in all three North Atlantic temperature records during the Pliocene (3.2 to 2.4 Ma) (Fig. 5A,B,C). This observation expands on the results of Medina-Elizalde and Lea (2010), who noted the presence of 100 kyr power during the "41 k world" in tropical SST records. While we note the absence of strong precessional power in most of these

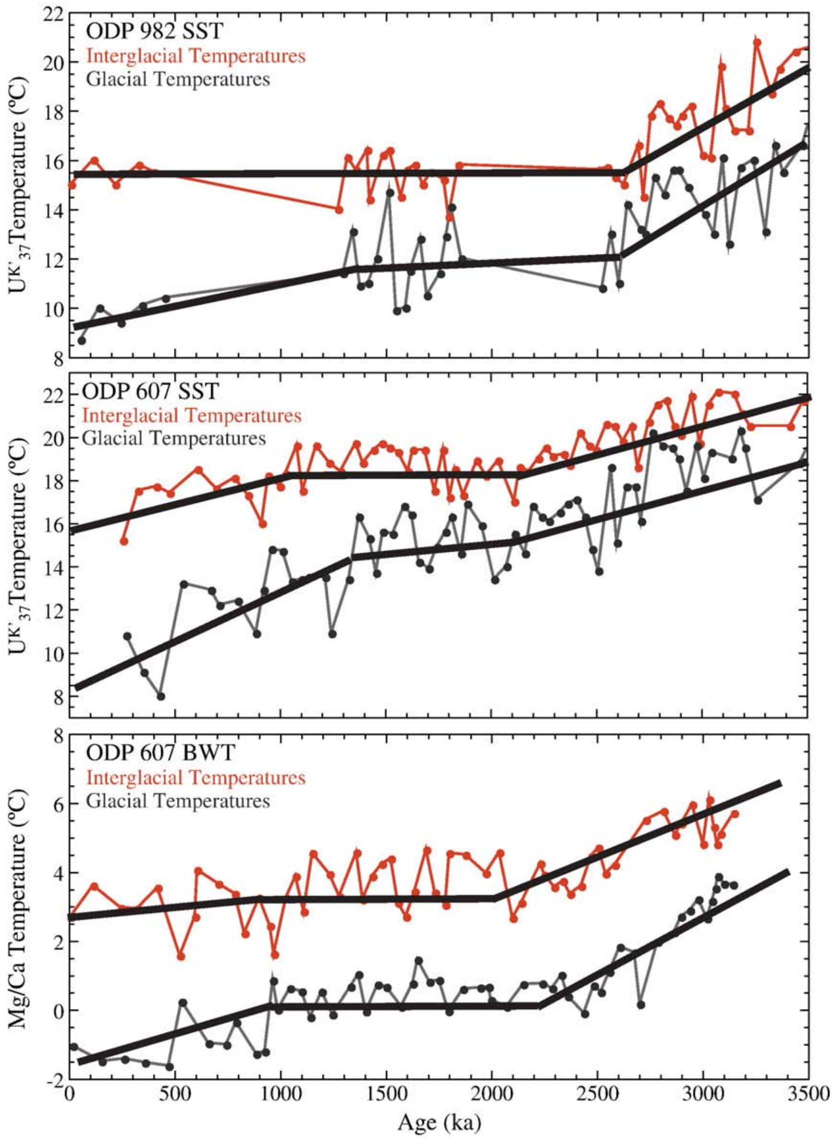

Fig. 4. Time series of glacial (gray dotted line) and interglacial (orange dotted line) extrema. Extrema for: A) Site 982 SST, B) Site 607 SST and C) Site 607 BWT. Points in each time series were determined by using glacial and interglacial intervals indentified in the LR04 stack (Lisiecki and Raymo, 2005) to select corresponding glacial and interglacial intervals in the SST time series. Dark black lines describe the general trends of these time series of extrema. Inflection points are based on calculated maximum rates of change for each individual time series. Note the symmetrical evolution of glacial and interglacial cooling during the LPT and the more pronounced cooling of glacial relative to interglacial intervals during the Pleistocene cooling step.

time series (Fig. 6), we acknowledge that the sampling resolution for our temperature time series (average resolution of ~3–4 kyr for DSDP 607 SST and BWT; ~10 kyr resolution for ODP 982 during intervals 2.5–1.75 Ma and 1.25–0.4 Ma) may miss some of the variance concentrated in this spectral band.

Orbital band phase relationships among our climate variables permit us to document the timing of North Atlantic climate responses relative to changes in orbital forcing and allow us to make inferences about regional versus global influences on North Atlantic climate. During the "41 kyr world" of the Pliocene and early Pleistocene, SST, BWT, and $\delta^{13}C$ responses in the dominant 41 kyr band are within error of being in phase with each other and lead by 2 kyr or less or are in phase with $\delta^{18}O_c$ (Fig. 7A, Table S1); the phasing of these 41 kyr band responses remains essentially the same during the late Pleistocene "100 kyr world" (Fig. 7B, Table S1). In contrast, North Atlantic climate responses in the 100 kyr band during the late Pleistocene, while strongly coherent, are not synchronous (Fig. 7C). In particular, BWT leads benthic $\delta^{18}O_c$ by 11 kyr ($\pm$5 at the 95%CI), whereas the other proxies are more closely in phase with each other and/or $\delta^{18}O_c$ (982 SST −5 kyr $\pm$ 2, 607 SST −3 kyr $\pm$ 5, and 607 $\delta^{13}C$ 3 kyr $\pm$ 5 relative to $\delta^{18}O_c$, where negative phases indicate a phase lead) (Fig. 7C, Table S1).

4. Discussion

4.1. Secular trends in North Atlantic climate

4.1.1. Late Pliocene transition

While cooling during the late Pliocene and early Pleistocene has long been evident from oxygen isotope records that span this interval (Lisiecki and Raymo, 2005), distinct regional patterns of cooling are only now becoming apparent with the emergence of high-resolution time series that provide independent constraints on past temperatures. The synthetic view of North Atlantic temperature evolution provided by the SST and BWT records examined here reveals two discrete phases of cooling during the past 3.2 Myr (Fig. 3). The nature of both of these cooling steps modifies our current understanding of Plio-Pleistocene climate change.

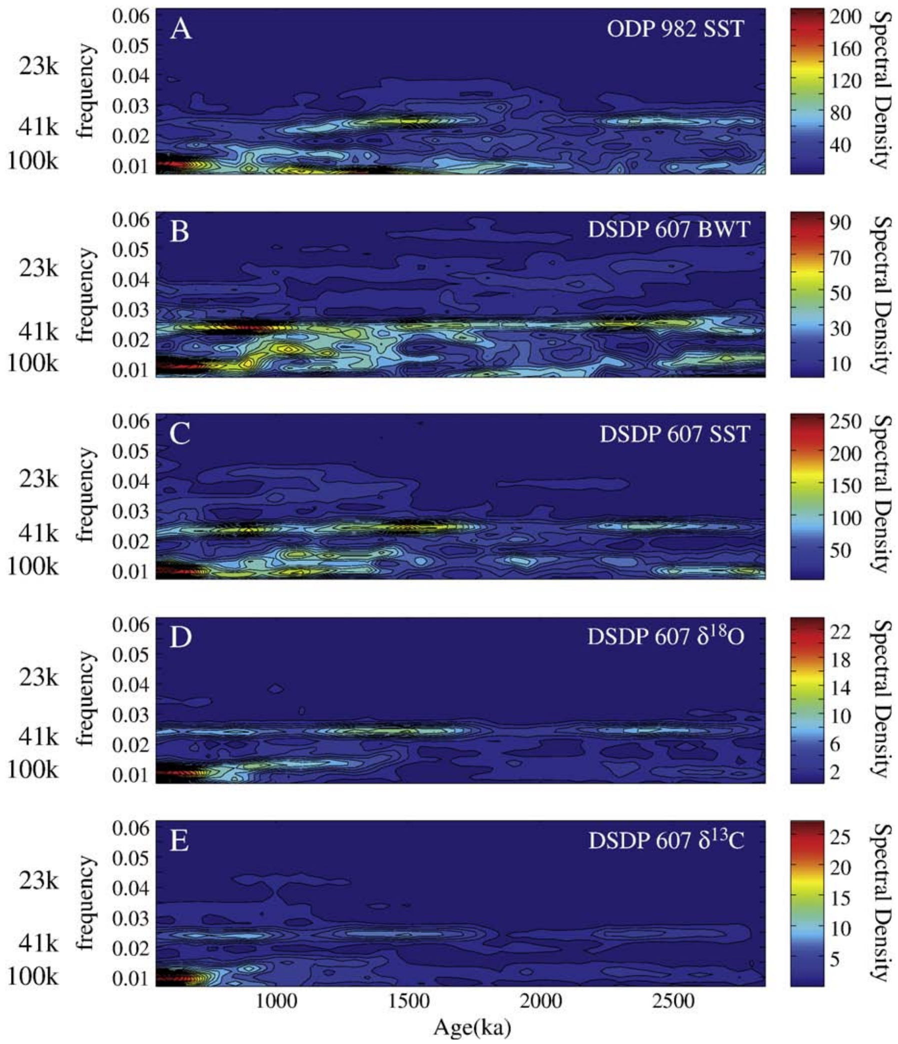

Fig. 5. Evolutionary spectra of paleoclimate time series. A) ODP Site 982 $U^{k'}_{37}$ SST (Lawrence et al., 2009) B) DSDP Site 607 Mg/Ca BWT (Sosdian and Rosenthal, 2009), C) DSDP Site 607 SST, D) DSDP Site 607 $\delta^{18}O_c$ (Raymo et al., 1989; Ruddiman et al., 1989; Raymo et al., 1992), and E) DSDP Site 607 $\delta^{13}C$ (Raymo et al., 1989; Ruddiman et al., 1989; Raymo et al., 1992). Spectra were computed using the Arand software (Howell, 2001) spectra program's iterative mode. All responses were interpolated to even intervals of 2 kyr resolution prior to analysis. Each plot is scaled to its own maximum spectra density. We applied a full linear detrend, the autocovariance function, a 600k window, 50% lags, and an increment of 75 kyr to each time series. Note due to constraints of time series length and selected window size, that the most recent data reported in these plots corresponds to 550 ka.

Most existing temperature (Dekens et al., 2007; Herbert et al., 2010; Lawrence et al., 2006; Wara et al., 2005) and $\delta^{18}O$ records spanning the Plio-Pleistocene suggest a gradual LPT cooling in comparison to the pronounced and discrete cooling step observed in the three temperature time series compared in this study (Fig. 3). Trends in Site 607 BWT and Site 982 SST indicate a nearly identical long-term evolution with similar timings and magnitudes of secular temperature change. If the BWT signal through much of the Plio-Pleistocene is derived primarily from the sinking of surface waters in the Nordic Seas as it is today, then it is not surprising that its long-term evolution is nearly identical to Site 982 SST, which records temperature variations in the surface ocean just south of the Nordic Seas. Whereas Site 607 SST shows the same two-stepped cooling pattern as Site 607 BWT and Site 982 SST, LPT cooling in the 607 SST record is larger in magnitude and delayed relative to the other two records (Fig. 3). We suggest that the higher amplitude and delayed response of 607 SST relative to the two other North Atlantic temperature time series is reasonably explained by its more southerly location at the northern edge of the North Atlantic gyre, further from the influence of high latitude processes. The equatorward shift of climate belts that occurred across the LPT (Brierley et al., 2009) likely changed climate conditions at Site 607 from being strongly subtropical to more subpolar. We suggest this shift can account for the larger amplitude temperature change observed in Site 607 SST relative to Site 982 SST and Site 607 BWT. The LPT cooling step in the Site 607 SST record ends ~0.4 Myr later than those in both the Site 982 SST and Site 607 BWT records. Presumably, as NH ice sheets progressively grew during the LPT, their influence on North Atlantic climate expanded resulting in a time transgressive growth of the NH polar region and a contraction of the temperate and subtropical climate belts to the south. We submit that the relative timing of initial SST cooling at 982 and 607 places a rough constraint on the rate of this process.

It is clear from time series of glacial and interglacial temperature extrema (Fig. 4) that at least in the North Atlantic a similar magnitude of cooling occurred in both glacial and interglacial intervals. This symmetric cooling of glacial and interglacial extrema suggests that the LPT was caused by a mechanism that induced a change in the mean climate state. The more pronounced cooling of the high latitude North Atlantic relative to lower latitude temperature records (i.e. 2–3 °C versus 0–2 °C, respectively) across the LPT (Fig. 4; Table 1) indicates an increase in the meridional temperature gradient suggesting that the mechanism responsible for this transition was either amplified in the North Atlantic (Herbert et al., 2010; Lawrence et al., 2006; Wara

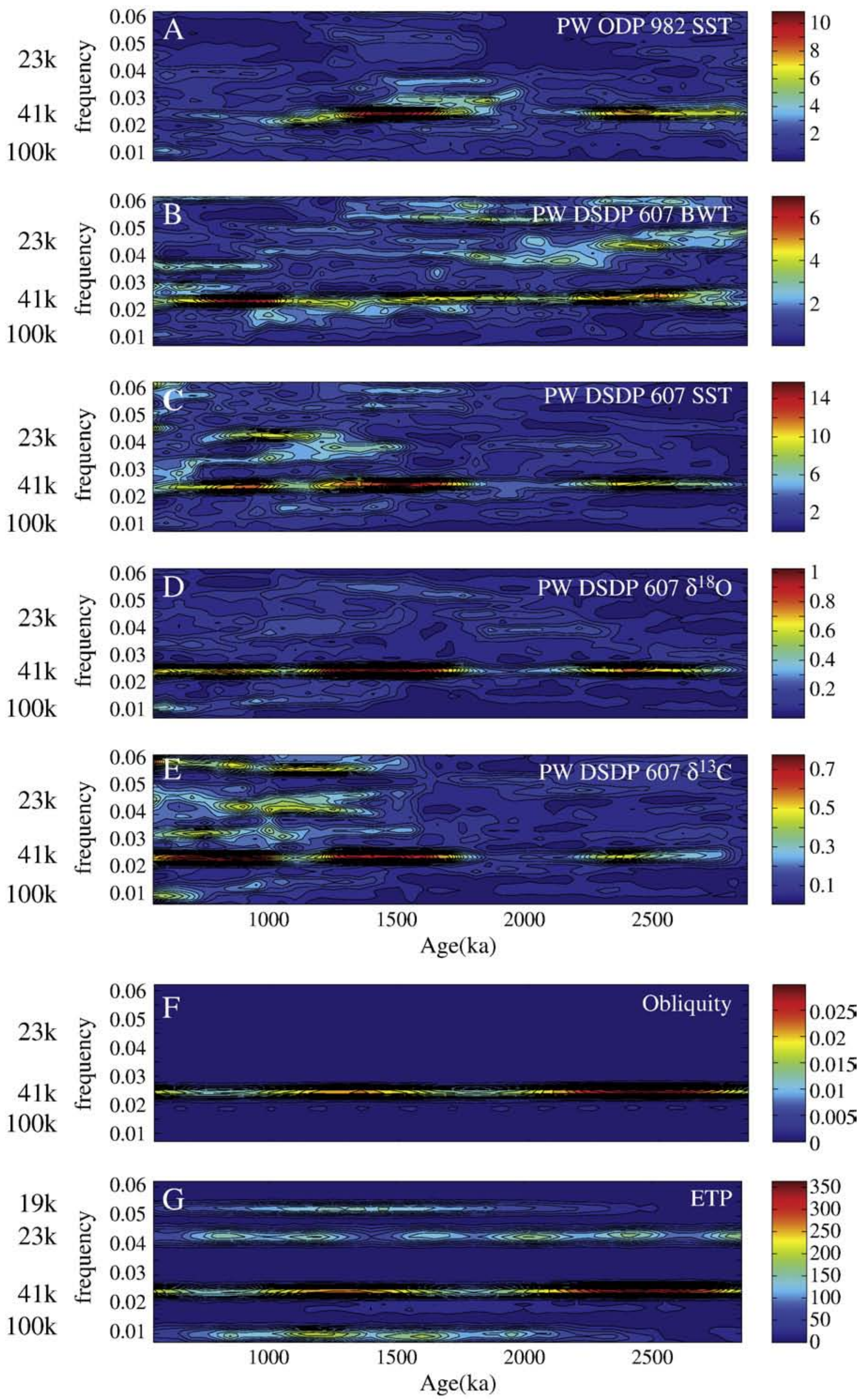

Fig. 6. Prewhitened (PW) evolutionary spectra of paleoclimate time series and evolutionary spectra of insolation forcing. A) ODP Site 982 $U^{k'}_{37}$ SST (Lawrence et al., 2009) B) DSDP Site 607 Mg/Ca BWT (Sosdian and Rosenthal, 2009), C) DSDP Site 607 SST, D) DSDP Site 607 $\delta^{18}O_c$ (Raymo et al., 1989; Ruddiman et al., 1989; Raymo et al., 1992), and E) DSDP Site 607 $\delta^{13}C$ (Raymo et al., 1989; Ruddiman et al., 1989; Raymo et al., 1992). Spectra were computed using the Arand software (Howell, 2001) spectra program's iterative mode. All responses were interpolated to even intervals of 2 kyr resolution prior to analysis. Each plot is scaled to its own maximum spectra density. We applied a full linear detrend, the autocovariance function, a 600k window, 50% lags, and an increment of 75 kyr to each time series. Time series were prewhitened by setting prewhitening equal to 1. Prewhitening attenuates spectra power produced by secular trends in the time series allowing for better resolution of higher frequency variations (e.g. 23 kyr and 41 kyr beat). We added spectra of F) obliquity (Laskar et al., 1993) and G) ETP (Imbrie et al., 1984) to allow for comparisons between orbital forcing and climate system responses. These time series were subjected to the same analysis as the time series above, but were not prewhitened. Note due to constraints of time series length and selected window size, that the most recent data reported in all plots in this figure corresponds to 550 ka.

et al., 2005) or that there was a reduction in poleward heat transport over time. A multi-proxy study comparing and contrasting mid-Pliocene versus modern SST estimates provides some evidence for the role of reduced heat transport in declining North Atlantic temperatures. Robinson et al. (2008) found much larger (2–6 °C greater) differences in North Atlantic SST estimates between the mid-Pliocene and modern from sites that underlie the North Atlantic Drift versus those that underlie regions outside of the current.

However, results from several recent studies prompt us to suggest that the consistent pattern of LPT cooling observed in North Atlantic

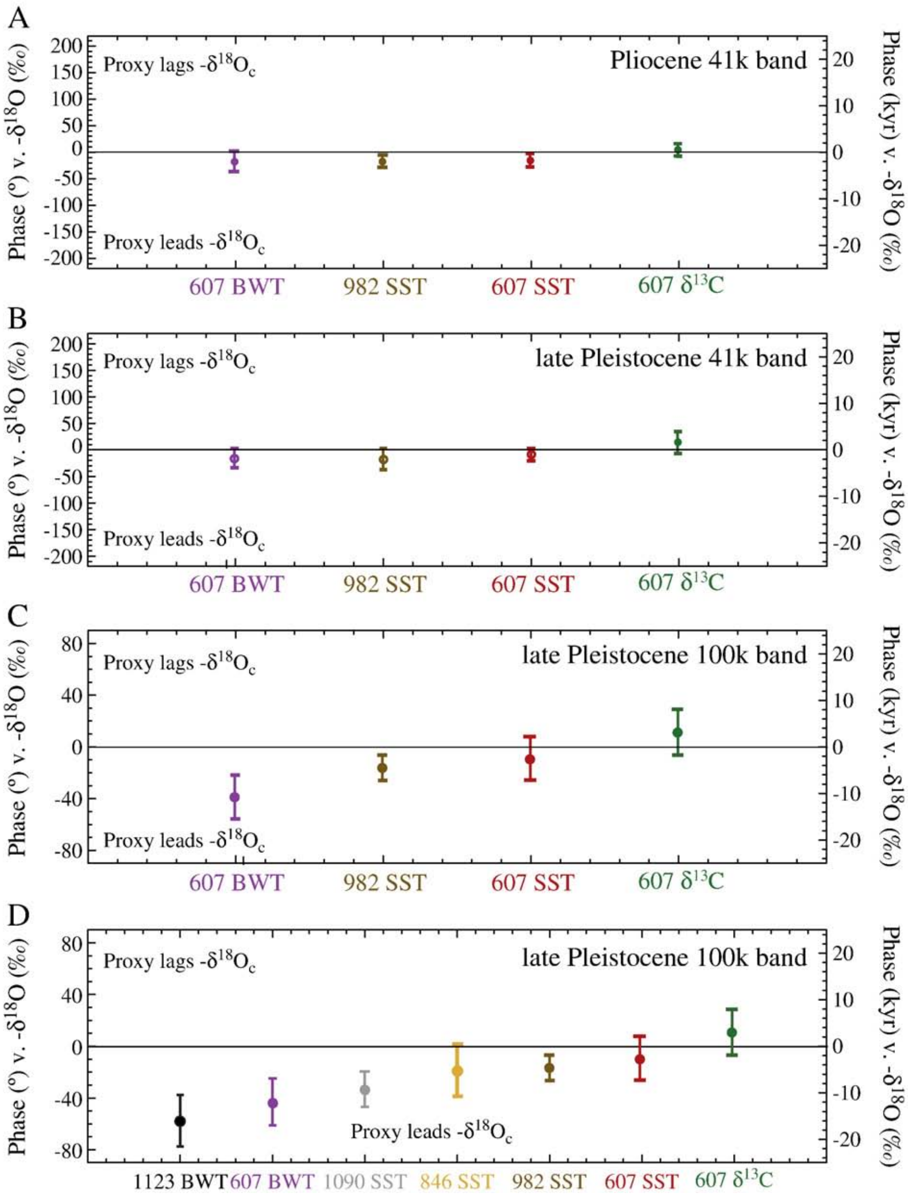

Fig. 7. Phase and coherency of each paleoclimate proxy relative to benthic $-\delta^{18}O_c$. A) North Atlantic responses during the late Pliocene "41k world" (2.7 to 2.2 Ma); B) North Atlantic responses in the 41 kyr band during the late Pleistocene "100k world" (0.75 Ma to 0.25 Ma); C) North Atlantic responses in the 100 kyr band during the late Pleistocene "100k world" (0.75 Ma to 0.25 Ma); and D) 100k band responses during the late Pleistocene "100k world" (0.75 Ma to 0.25 Ma) (Elderfield et al., 2009; Lawrence, 2006; Lawrence et al., 2009; Martinez-Garcia et al., 2009). Responses that are coherent at the 80% confidence level are shown as empty circles, while those that are coherent at the 95% confidence level are shown with solid circles. However, note that from the phase estimates reported in Elderfield et al. (2009) it is unclear whether the 100 kyr phase relationship between Site 1123 BWT and $\delta^{18}O_c$ is at the 80% or 95% confidence level. We used the inverse of benthic $\delta^{18}O_c$ to be consistent with paleoclimatic convention. We used the Arand software (Howell, 2001) Crospec program's iterative mode with a 500k window, 250k lags, and a 50k increment to compute all phases. We interpolated all records to even intervals of 3 kyr resolution prior to phase and coherency analysis.

temperature records was most plausibly initiated by a decrease in atmospheric pCO_2 and an associated strong regional ice albedo feedback. Despite significant uncertainties associated with each of the many methodologies that have been used to produce past estimates of Pliocene pCO_2, virtually all estimates converge on early to mid-Pliocene carbon dioxide concentrations ~50–150 ppm higher than pre-industrial values (280 ppm) (Kürschner et al., 1996; Pagani et al., 2009; Raymo et al., 1996; Seki et al., 2010; Tripati et al., 2009; Van Der Burgh et al., 1993). The most detailed of these reconstructions across the LPT (Seki et al., 2010) shows a decline in pCO_2 between ~3.1 and 2.8 Ma, coeval with the strong cooling step evident in the North Atlantic temperature records presented here (Fig. 3). Recently published paleoclimate modeling research examining the sensitivity of Greenland ice growth to changes in pCO_2 suggests that pCO_2 changes of this magnitude may have been critical to the LPT (DeConto et al., 2008; Lunt et al., 2008). These studies found strong sensitivity of the Greenland ice sheet to the range of pCO_2 values between those documented by Pliocene pCO_2 studies and pre-industrial concentrations (280 ppm). The modest change in late Pliocene pCO_2 (Pagani et al., 2009; Tripati et al., 2009) coincides with the appearance of strong evidence for significant ice growth (Lawrence et al., 2009; Mudelsee and Raymo, 2005). Using Site 607 $\delta^{18}O$ and Mg/Ca BWT records, Sosdian and Rosenthal (2009) estimate a gradual decrease in mean sea level of about ~22 m ($\pm$21 m) associated with the shift in mean climate state across the LPT. Ice-rafted debris records from the North Atlantic suggest major changes in NH ice volume at this time, particularly in Greenland (Jansen et al., 2000; Larsen et al., 1994; Raymo et al., 1989; Raymo et al., 1986; Shackleton et al., 1984; St. John and Krissek, 2002). These results, along with our North Atlantic temperature records, suggest that once ice sheets appeared in the NH a strong ice albedo feedback amplified cooling regionally. Taken together these recent findings suggest that although the pCO_2 change between the Pliocene and modern was likely quite modest, that change may have pushed the climate system across an important threshold in which the North Atlantic region became cool enough to accommodate the growth of a sizeable Greenland ice sheet during the LPT. It is noteworthy however, that the decreasing pCO_2/albedo feedback and heat transport mechanisms used to explain late Pliocene cooling of the North Atlantic are not mutually exclusive. The gradual growth of a sizeable ice sheet in Greenland in response to falling atmospheric CO_2 concentrations, would not only impact regional SST but would also affect the strength and position of atmospheric pressure cells and thus the strength and paths of atmospheric and oceanic heat transport.

4.1.2. Mid-Pleistocene transition

The defining characteristics of the MPT are an increase in the amplitude of glacial–interglacial cycles and a shift in the dominant periodicity of these cycles from 41 kyr to 100 kyr in climate time series that span the Pleistocene (Clark et al., 2006; Clark and Pollard, 1998; Imbrie et al., 1992, 1993). Our temperature synthesis indicates that like the LPT, the MPT is associated with temperature change in the North Atlantic (Figs. 2, 5, 6); a significant cooling (1.5 to 2.5 °C) commenced in the North Atlantic ~1.5 to 1.3 Ma, just prior to the start of the MPT (Fig. 3). However, in contrast with the LPT, the MPT is also associated with a substantial change in Atlantic meridional ocean circulation as evident in changes in both the secular trend and magnitude of glacial–interglacial variability of the benthic foraminiferal $\delta^{13}C$ record (Figs. 2, 3). Thus, the characteristics and likely causes of the cooling associated with the MPT may be different from that of the LPT. Examination of trends in glacial and interglacial extrema over the past 2 Myr shows that this cooling was preferentially driven by a progressive decrease in glacial temperatures with much smaller temperature changes occurring during interglacials (Fig. 4). This salient feature of the North Atlantic temperature time series is also evident in Pleistocene temperature time series from both coastal and tropical upwelling zones (Brierley et al., 2009; Dekens et al., 2007; Etourneau et al., 2009; Herbert et al., 2010; Liu and Herbert, 2004), but is absent in temperature records from the Western Pacific Warm Pool (WPWP) (de Garidel-Thoron et al., 2005; Medina-Elizalde and Lea, 2005). These patterns provide clues about the kind of mechanism potentially responsible for the MPT. They demand that the mechanism account for significant cooling in high latitude regions (which also plumb waters into lower latitude upwelling regions) before the strong frequency and amplitude shifts that characterize the MPT. In addition, they suggest that the cooling must be driven by a process that preferentially occurs during glacial intervals.

Both groups of mechanisms previously invoked to explain the MPT, a long-term cooling ("cooling hypothesis") in response to a change in atmospheric pCO_2 and a change in ice sheet dynamics ("regolith hypothesis"), have some merit in accounting for the observed temperature patterns. There is an absence of evidence to support a secular drawdown of CO_2 across the MPT (Seki et al., 2010), but some preliminary evidence to suggest there may have been a change in CO_2 drawdown during glacial intervals (Hönisch et al., 2009). Using boron isotope based estimates of past glacial–interglacial variations in pCO_2, Honisch et al. (2009) assert that while pCO_2 concentrations during interglacial periods remained essentially unchanged, a small (~30 ppm) decrease in glacial pCO_2 values occurred across the MPT. This dataset implies an asymmetry in greenhouse gas forcing that matches the pattern of temperature change observations from most existing temperature records that span this transition, including our North Atlantic sites and upwelling zones in both coastal and tropical regions (Brierley et al., 2009; Dekens et al., 2007; Etourneau et al., 2009; Herbert et al., 2010; Liu and Herbert, 2004). Thus, a change in atmospheric pCO_2 during glacial times could potentially account for the asymmetric cooling we observe in our North Atlantic datasets. Two conceivable mechanisms for this glacial CO_2 linkage are glacial changes in the mid to high latitude wind field and/or high latitude sea ice extent. Both of these mechanisms should cause changes in ventilation that could lead to the sequestration of additional CO_2 in the deep ocean during glacial times (Toggweiler et al., 2006). However, significant uncertainties are associated with all methodologies for estimating past pCO_2. In addition, unless the changes in pCO_2 across the MPT were so small that they were below the sensitivity threshold for temperature change in the Western Pacific Warm Pool (WPWP), the absence of any notable change in mean SST or glacial SST in the WPWP associated with the MPT (de Garidel-Thoron et al., 2005; Medina-Elizalde and Lea, 2005) challenges the validity of the CO_2 mechanism. Furthermore, this mechanism also fails to explain geological observations from terrestrial till deposits, which suggest that pre-MPT NH ice sheets covered a similar or larger area than those that existed after the MPT (Balco et al., 2005; Roy et al., 2004).

In contrast, Clark and Pollard (1998) invoke physical processes associated directly with the ice sheets to explain the shift into the late Pleistocene 100 kyr regime. The so called "regolith hypothesis" attributes the MPT to an increase in ice sheet thickness and the development of instabilities at the margin of these ice sheets in response to a gradual change in ice sheet substrate from soft, low friction regolith to a harder, high friction crystalline bedrock (Clark et al., 2006; Clark and Pollard, 1998). In addition to being able to explain the amplitude and frequency shifts that characterize the MPT, this hypothesis can account for geologic observations that suggest that pre-MPT and post-MPT ice sheets had similar areal extents (Balco et al., 2005; Roy et al., 2004). The influence of thicker ice sheets on North Atlantic climate through changes in atmospheric circulation and sea ice extent could plausibly account for cooling across the MPT (Ganopolski et al., 1998; Manabe and Broccoli, 1985). Augmented sea ice during glacial intervals and the potential affect of sea ice extent on the communication of CO_2 between the atmosphere and ocean could provide the positive feedbacks necessary to explain the preferential cooling observed during glacial intervals associated with the MPT. However, while we observe the growth of a broad low frequency band of (80–100 kyr) variance in the evolutionary spectra from our North Atlantic temperature records that occurs at about the same time of the observed late Pleistocene cooling and previous studies indicate an early shift in the southward extent of subarctic water masses (~1.2 Ma) and the position of the Arctic frontal position (~1 Ma) particularly during glacial intervals (McClymont et al., 2008; Wright and Flower, 2002), the MPT amplitude and frequency shift in the $\delta^{18}O$ (ice volume) record develops after the start of the cooling step and observed movements in the polar front (Figs. 3, 5). Thus, it seems unlikely that the MPT can be explained by changes in ice sheet dynamics alone. We conclude that the MPT might not solely be explained by one or the other of these hypotheses, but rather some combination of them. Further evidence documenting past pCO_2 variability and ice sheet dynamics are required to understand the ultimate cause of the MPT.

4.2. Orbital phasing among climatic responses

The orbital-resolution Plio-Pleistocene datasets we examine here enable us to expand upon and in some cases revise the groundbreaking work of the SPECMAP Project (Imbrie et al., 1992, 1993). While SPECMAP examined the relationship among climate variables during the colder, 100 kyr climate regime of the late Pleistocene, the work conducted here allows us to explore the timing of climate system responses during a markedly different climate regime — the warmer and 41 kyr dominated world of the Pliocene. Our analysis indicates a consistent and highly coherent phase response of North Atlantic SST, BWT, and $\delta^{13}C$ during the Pliocene suggesting that all of these climate signals were imparted in the North Atlantic (Fig. 7A). We interpret the slight phase lead of North Atlantic temperature records relative to

$\delta^{18}O_c$ as an indication of the relative response times of these components to insolation forcing, where the high inertia of the ice sheets should lag the rapid response of the ocean surface. The same phase relationships in the 41 kyr band also persist throughout the Pleistocene suggesting that within the 41 kyr band climate evolution during the Pleistocene did not influence the North Atlantic climate system's response to obliquity forcing (Fig. 7A,B). While for clarity of presentation, we show phase relationships for only two representative time slices (Figs. 7A,B), these relationships hold throughout the duration of these climate records. In contrast, in the late Pleistocene 100k band, we find coherent but not synchronous NH climate system responses to forcing (Fig. 7C), which indicate that the sequence of late Pleistocene North Atlantic climate responses in the 100 kyr band was different than in the 41 kyr band. Specifically, we find that the 607 BWT response leads $\delta^{18}O_c$, the SST record from Site 982 lags the 607 BWT response but leads $\delta^{18}O_c$, 607 SST responds in phase with $\delta^{18}O_c$, and 607 $\delta^{13}C$ is in phase with or slightly lags the oxygen isotope signal. These results build on the recent findings of Lisiecki et al. (2008), who determined that the phasing of the ocean circulation response during the late Pleistocene, as recorded by $\delta^{13}C$, was distinctly different in the 41 kyr and 23 kyr bands. Both of these findings call into question the SPECMAP conclusion that the late Pleistocene climate system response was the same in all three orbital bands (Imbrie et al., 1992, 1993).

Observations from our own datasets, as well as recent contributions by others (Elderfield et al., 2009; Lisiecki et al., 2008; Martinez-Garcia et al., 2009; Stott et al., 2007), compel us to propose a new model to explain the relative timing of North Atlantic climate system responses during the late Pleistocene. We note that the 100 kyr band response of Site 607 BWT during the late Pleistocene clearly leads the Site 607 $\delta^{13}C$ record (Fig. 7C). The benthic foraminiferal glacial–interglacial $\delta^{13}C$ records at DSDP 607 and nearby sites have been typically interpreted as reflecting, to a large extent, variations in the relative contributions of the relatively warm, salty, and nutrient depleted NADW versus the cold, relatively fresh, and nutrient enriched AABW (Raymo et al., 1997). We acknowledge that changes in source water properties (i.e. air–sea gas exchange) and/or local productivity (i.e. flux of algal detritus from surface ocean) could also potentially influence the Site 607 $\delta^{13}C$ signal, in which case the $\delta^{13}C$ phasing may not solely represent changes in ocean circulation. However, we think these influences are unlikely the primary explanation for the observed phase relationships. Changes in air–sea gas exchange, specifically exposure to colder temperatures, would drive the $\delta^{13}C$ to more positive values in contrast to the observations. Furthermore, since the lead of $\delta^{13}C$ relative to $\delta^{18}O$ is not unique to Site 607, as this result is reproduced by a similar analysis at ODP Site 659 (18°N, 21°W, water depth 2532 m), and is also corroborated by several other studies from the North Atlantic, we do not think that local productivity changes influenced the phasing of the $\delta^{13}C$ signal (Flower et al., 2000; Lisiecki et al., 2008; Skinner and Shackleton, 2006).

Changes in deep ocean circulation, as inferred from sediment cores in the North Atlantic, have been linked to surface temperature in North Atlantic high latitude regions (Boyle and Keigwin, 1987). However, if the 100 kyr band Site 607 BWT and $\delta^{13}C$ signals were both imparted in the North Atlantic, then presumably the Site 982 and 607 SST records, from locations proximal to NADW formation regions should show a phase lead similar to that of BWT relative to benthic $\delta^{18}O_c$. Yet, our data clearly indicate that this is not the case (Fig. 7C). While phases of both SST records do lead $\delta^{18}O_c$, these phase differences are consistent with the expected difference in response times of these climate components to changes in insolation forcing, with the rapidly responding sea surface changing 3 to 5 kyr before the sluggishly responding ice sheets. The early 607 BWT response during the late Pleistocene relative to the 607 $\delta^{13}C$ response indicates that changes in North Atlantic deepwater temperature were not synchronized with NADW formation in the North Atlantic, suggesting that these signals were derived from different source regions. We propose that changes in Site 607 BWT on 100 kyr timescales were imparted not from the North Atlantic, but from the other region that is plumbed to the deep Atlantic Ocean — the high latitudes of the southern hemisphere.

The phasing of other southern hemisphere proxy records relative to benthic $\delta^{18}O_c$ supports our inference that the large lead of BWT over all other northern hemisphere proxies in “100 k world” is a result of a southern hemisphere influence. Both the BWT record of Elderfield et al. (2009) from Chatham Rise Site 1123 (42°S, 171°W, 3290 m) and the SST record of Martinez-Garcia et al. (2009) from South Atlantic Site 1090 (43°S, 9°W, 3700 m) (Fig. 1) show substantial leads over $\delta^{18}O_c$ in the 100 kyr band (Fig. 7D). The lead of 607 BWT over $\delta^{18}O_c$ observed in our analysis, corroborates the work of Shackleton (2000), who also estimated an early deep ocean temperature response. Similarly, results from the SPECMAP project indicate that southern hemisphere proxies in all bands were recorded as “early responses” whereas NH proxies yielded “late responses” relative to $\delta^{18}O_c$ (Imbrie et al., 1992, 1993; Shackleton, 2000). Furthermore, a recent high-resolution study spanning the last deglacial period also demonstrates that the early climate system responses to orbital forcing occur in the southern hemisphere (Stott et al., 2007).

The large lead of BWT changes over $\delta^{13}C$ changes (~12 kyr) develops in association with the MPT amplitude and frequency shift (Figs. 2, 5, 8). In addition to the development of this unique phasing, a major reorganization in the North Atlantic overturning circulation occurred across the MPT. Specifically, during glacial periods, NADW (high $\delta^{13}C$) became suppressed and the influence of southern source waters, specifically AABW (low $\delta^{13}C$), in the deep North Atlantic increased as is evident from the increase in the glacial–interglacial

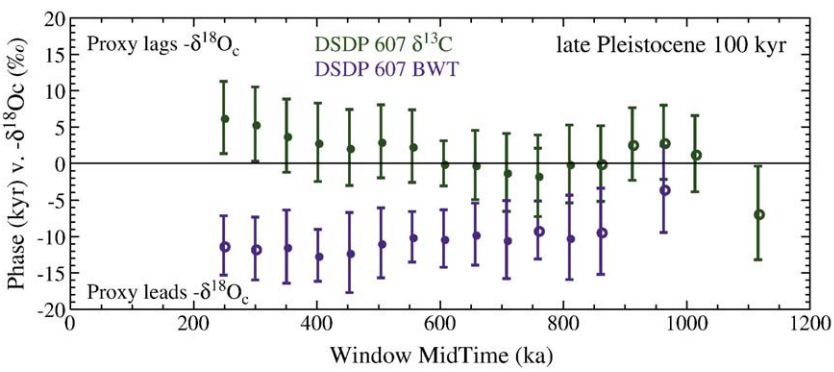

Fig. 8. Late Pleistocene phasing of climate system responses. DSDP Site 607 phase and coherency between BWT, $\delta^{13}C$ and benthic $-\delta^{18}O_c$. Intervals that are coherent at the 80% confidence level are shown as empty circles, those that are coherent at the 95% confidence level are shown with solid circles. We used the inverse of benthic $\delta^{18}O_c$ in our coherency and phase analyses, to be consistent with paleoclimatic convention. Prior to coherency and phase analysis all records were interpolated to even intervals of 3 kyr resolution. We used the Arand software (Howell, 2001) Crospec program's iterative mode with a 500k window, 250k lags, and a 50k increment to compute all phases.

amplitude of the 607 $\delta^{13}C$ time series and the dramatic change in absolute value of $\delta^{13}C$ across this transition (Raymo et al., 1997; Venz and Hodell, 2002) (Figs. 2E, 3B). Thus, the $\delta^{13}C$ time series indicates that across the MPT Site 607 shifted from dominantly being ventilated by NADW to being ventilated by AABW, a southern watermass, during glacial periods. In the modern ocean, AABW forms during the winter largely along the margins of West Antarctic Ice Sheet (WAIS). When sea ice forms in the Weddell Sea, Ross Sea, and off Wilkes Land, brine rejection occurs and affects the surface ocean salinity and thus deepwater formation. On orbital time scales, insolation induced changes in the extent of the WAIS could vary the sea ice margins in these regions (England, 1992; Seidov et al., 2001; Stocker et al., 1992) and thus play an important role in governing AABW formation.

Evidence from the ANDRILL project shows that major changes in the extent of the WAIS driven by orbital changes in insolation occurred during the Plio-Pleistocene, with a progression towards a much more continuously glaciated state in the Pleistocene (Naish et al., 2009). A study using an ice sheet model to explore the waxing and waning of the WAIS over the past 5 Myr, shows that the different sectors of the WAIS tend to respond in unison (Pollard and DeConto, 2009), suggesting that the history of ice sheet growth and decay from the Ross embayment recorded by the ANDRILL project is representative of the entire WAIS and surrounding seas. We propose that the establishment of a more extensive WAIS across the MPT may have affected production of deep water masses in the Southern Ocean, specifically the export of AABW, via changes in ice shelves and associated brine rejection. We suggest that prior to the MPT, the WAIS was too small to affect AABW production or that the extent of AABW in the deep North Atlantic was limited to regions south of Site 607. As global temperatures decreased over the Plio-Pleistocene a more extensive WAIS ice sheet and associated ice shelves acted to increase the ventilation of Southern Ocean deep waters and exert a stronger influence on the deep North Atlantic.

We attribute the unique phasing we observe between Site 607 BWT and $\delta^{13}C$ after the MPT to processes occurring in different hemispheres. After the MPT, Site 607 is dominated during glacial intervals by the influence of AABW, as reflected in by low $\delta^{13}C$ values. The early phasing of 607 BWT relative to $\delta^{13}C$ and $\delta^{18}O$, and its synchroneity with SST changes in the Southern Ocean suggest that physical changes in bottom water properties at this site are tightly linked to Southern Ocean processes. In contrast, the phasing of $\delta^{13}C$ is dictated by NADW production, which is strongly tied to the high inertia of NH ice and reflects the reintroduction of nutrient depleted NADW into the North Atlantic at the end of glacial cycles. Prior to the MPT, we posit that the smaller size of the WAIS ice sheet limited the amount and influence of AABW formation. This conclusion is supported by the differing responses we observe in the 41 kyr versus 100 kyr bands. Across the Plio-Pleistocene, NH proxy records are tightly linked to NH processes in the 41 kyr band. Obliquity driven changes in North Atlantic temperature and NADW are synchronous and support the notion that in the 41 kyr band NADW predominantly resides at Site 607 with minimal AABW intrusion. We suggest that the unique phasing between Site 607 BWT and $\delta^{13}C$ develops in the 100k band in the "100 kyr world" in response to large swings in southern source water due to the development of a more extensive WAIS. This mechanism highlights a potentially important role for the WAIS in driving changes in ocean circulation and climate and suggests that after the MPT both NH and southern hemisphere ice sheets exerted a significant influence on far afield climate conditions.

5. Conclusions

We observe remarkably consistent responses among North Atlantic climate proxies on both secular and orbital timescales, which suggests a coordinated regional response to changes in climate forcing. Our temperature synthesis reveals that two distinct cooling steps occurred over the past 3.2 Myr, one during the late Pliocene and the other during early to mid-Pleistocene. Cooling during the late Pliocene occurred symmetrically during both glacial and interglacial intervals indicating that these changes were caused by a change in the mean climate state. We suggest that these observations of North Atlantic temperature change are most consistent with a thresholded ice albedo response to declining atmospheric CO_2 during the LPT. In contrast, North Atlantic temperature change in the Pleistocene was characterized by preferential cooling during glacials and began before the heart of the frequency shift and amplitude increase that define the MPT. This antecedent cooling suggests that a change in ice sheet dynamics may not be the sole explanation for the MPT and that some other mechanism, potentially a decline in glacial pCO_2, is necessary to account for the observed changes. On orbital timescales, the coherency and synchroneity in the 41 kyr band among North Atlantic climate proxies and deepwater properties imply that 41 kyr responses during the Pliocene and the late Pleistocene were driven by NH climate processes. After the MPT, however, 100 kyr climate responses in the North Atlantic, while strongly coherent, were not synchronous. Our results suggest that after the MPT the controls on deep ocean temperature and circulation changes are decoupled. We propose that the expansion of the WAIS across the MPT increased the production and export of AABW from the Southern Ocean, particularly during glacial intervals. If this hypothesis is correct, the early 100 kyr response of BWT suggests an early response of the WAIS relative to the NH ice sheets. However, the re-establishment of modern type deep ocean circulation during interglacial intervals is linked to the NH deglaciation.

Supplementary materials related to this article can be found online at doi:10.1016/j.epsl.2010.10.013.

Acknowledgements

We thank the Ocean Drilling Program for providing the sediment samples used in this analysis. We are grateful for productive and insightful conversations about this work with T. Herbert, L.C. Peterson, R. Toggweiler, J. Wright, D. Sigman, C.A. Riihimaki, and L. Lisiecki. We acknowledge support for this work from NSF grant # OCE0623310 to K.T.L. and an ODP Schlanger Fellowship to S.S.

References

Balco, G., Rovey II, C.W., Stone, J.O.H., 2005. The first glacial maximum in North America. Science 307, 222.
Berger, A., Li, X.S., Loutre, M.F., 1999. Modeling northern hemisphere ice volume over the last 3 Ma. Quaternary Science Reviews 18, 1–11.
Boyle, E.A., Keigwin, L.D., 1982. Deep circulation of the North Atlantic over the last 200,000 years: geochemical evidence. Science 218 (4574), 784–787.
Boyle, E.A., Keigwin, L.D., 1985/86. Comparison of Atlantic and Pacific paleochemical records for the last 215,000 years: changes in deep ocean circulation and chemical inventories. Earth and Planetary Science Letters 76, 135–150.
Boyle, E.A., Keigwin, L.D., 1987. North Atlantic thermohaline circulation during the last 20,000 years linked to high latitude surface temperature. Nature 330, 35–40.
Brassell, S.C., Eglinton, G., Marlowe, I.T., Pflaumann, U., Sarnthein, M., 1986. Molecular stratigraphy: a new tool for climatic assessment. Nature 320, 129–133.
Brierley, C.M., Fedorov, A.V., Liu, Z., Herbert, T.D., Lawrence, K.T., LaRiviere, J.P., 2009. Greatly expanded tropical warm pool and weakened Hadley circulation in the early Pliocene. Science 323, 1714–1718.
Cane, M.A., Molnar, P., 2001. Late Cenozoic closing of the Indonesian seaway as the missing link between the Pacific and East African aridification. Nature 411, 157–162.
Clark, P.U., Pollard, D., 1998. Origin of middle Pleistocene transition by ice sheet erosion of regolith. Paleoceanography 13 (1), 1–9.
Clark, P.U., Archer, D., Pollard, D., Blum, J.D., Rial, J.A., Brovkin, V., Mix, A.C., Pisias, N.G., Roy, M., 2006. The middle Pleistocene transition: characteristics, mechanisms, and implications for long-term changes in atmospheric pCO_2. Quaternary Science Reviews 25, 3150–3184.
Cleaveland, L.C., Herbert, T.D., 2007. Coherent obliquity band and heterogeneous precession band responses in early Pleistocene tropical sea surface temperatures. Paleoceanography 22, PA2216. doi:10.1029/2006PA001370.
de Garidel-Thoron, T., Rosenthal, Y., Bassinot, F.C., Beaufort, L., 2005. Stable sea surface temperatures in the western Pacific warm pool over the past 1.75 million years. Nature 433, 294–298.
DeConto, R.M., Pollard, D., Wilson, P.A., Palike, H., Lear, C.H., Pagani, M., 2008. Thresholds for Cenozoic bipolar glaciation. Nature 455, 652–656.

Dekens, P.S., Ravelo, A.C., Mc Carthy, M.D., 2007. Warm upwelling regions in the Pliocene warm period. Paleoceanography 22, PA3211. doi:10.1029/2206PA001394.

Driscoll, N.W., Haug, G., 1998. A short circuit in thermohaline circulation: a cause for northern hemisphere glaciation. Science 282, 436–438.

Elderfield, H., Greaves, M., Barker, S., Hall, I.R., Tripati, A., Ferretti, P., Crowhurst, S., Booth, L., Daunt, C., 2009. A record of bottom water temperature and seawater ∂18O for the Southern Ocean over the past 440 kyr based on Mg/Ca of benthic foraminiferal Uiverina spp. Quaternary Science Reviews 10.1016/j.quascirev.2009.1007.1013.

England, M.H., 1992. On the formation of Atlantic intermediate and bottom water in ocean general circulation models. Journal of Physical Oceanography 22, 918–926.

Etourneau, J., Martinez, P., Blanz, T., Schneider, R., 2009. Pliocene–Pleistocene variability of upwelling activity, productivity, and nutrient cycling in the Benguela region. Geology 37, 871–874.

Flower, B.P., Oppo, D.W., McManus, J.F., Venz, K.A., Hodell, D.A., Cullen, J.L., 2000. North Atlantic intermediate to deep water circulation and chemical stratification during the past 1 Myr. Paleoceanography 15 (4), 388–403.

Ganopolski, A., Rahmstorf, S., Petoukhov, V., Claussen, M., 1998. Simulation of modern and glacial climates with a coupled global model of intermediate complexity. Nature 391, 351–356.

Haug, G.H., Tiedemann, R., 1998. Effect of the formation of the Isthmus of Panama on Atlantic Ocean thermohaline circulation. Nature 393, 673–676.

Herbert, T.D., Peterson, L.C., Lawrence, K.T., Liu, Z., 2010. Tropical ocean temperatures over the past 3.5 Myr. Science.

Hönisch, B., Hemming, N.G., Archer, D., Siddall, M., McManus, J., 2009. Atmospheric carbon dioxide concentration across the mid-Pleistocene transition. Science 324, 1551–1554.

Howell, P., 2001. ARAND Time Series and Spectral Analysis Package for the Macintosh, in IGBP PAGES/World Data Center for Paleoclimatology Data Contribution, edited. NOAA/NGDC Paleocliamtology Program, Boulder, CO.

Imbrie, J., Hays, J.D., Martinson, D.G., McIntyre, A., Mix, A.C., Morley, J.J., Pisias, N.J., Prell, W.L., Shackleton, N.J., 1984. The orbital theory of Pleistocene climate. In: Berger, A., Reidel, D., Norwell, M.A. (Eds.), Support from a Revised Chronology of the Marine δ^{18}O Record, in Milankovitch and Climate, Part I.

Imbrie, J., Boyle, E.A., Clemens, S.C., Duffy, C., Howard, W.R., Kukla, G.J., Kutzbach, J.E., Martinson, D.G., McIntyre, A., Mix, A., Molfino, B., Morley, J.J., Peterson, L.C., Pisias, N.G., Prell, W.L., Raymo, M.E., Shackleton, N.J., Toggweiler, J.R., 1992. On the structure and origin of major glaciation cycles 1. Linear responses to Milankovitch forcing. Paleoceanography 7 (6), 701–738.

Imbrie, J., Berger, A., Boyle, E.A., Clemens, S.C., Duffy, C., Howard, W.R., Kukla, G., Kutzbach, J.E., Martinson, D.G., McIntyre, A., Mix, A., Molfino, B., Morley, J.J., Peterson, L.C., Pisias, N., Prell, W.L., Raymo, M.E., Shackleton, N.J., Toggweiler, J.R., 1993. On the structure and origin of major glaciation cycles 2. The 100,000-year cycle. Paleoceanography 8 (6), 699–735.

Jansen, E., Fronval, T., Rack, F., Channell, J.E.T., 2000. Pliocene–Pleistocene ice rafting history and cyclicity in the Nordic Seas during the last 3.5 Myr. Paleoceanography 15 (6), 709–721.

Kürschner, W.M., Van Der Burgh, J., Visscher, H., Dilcher, D.L., 1996. Oak leaves as biosenors of late Neogene and early Pleistocene paleoatmospheric CO_2 concentrations. Marine Micropaleontology 27, 299–312.

Larsen, H.C., Saunder, A.D., Clift, P.D., Beget, J., Wei, W., Spezzaferri, S., 1994. Seven million years of glaciation in Greenland. Science 264 (5161), 952–955.

Laskar, J., Joulet, F., Boudin, F., 1993. Orbital, precessional, and insolation quantities for the earth from −20 Myr to +10 Myr. Astronomy & Geophysics 270, 522–533.

Lawrence, K. T. (2006), Characterizing the Plio-Pleistocene evolution of sea surface conditions using the alkenone organic proxy, PhD thesis, 268 pp, Brown University, Providence, RI.

Lawrence, K.T., Liu, Z., Herbert, T.D., 2006. Evolution of the eastern tropical Pacific through Plio-Pleistocene glaciation. Science 312, 79–83.

Lawrence, K.T., Herbert, T.D., Brown, C.M., Raymo, M.E., Haywood, A.M., 2009. High-amplitude variations in North Atlantic sea surface temperature during the early Pliocene warm period. Paleoceanography 24. doi:10.1029/2008PA001669.

Lisiecki, L.E., Raymo, M.E., 2005. A Pliocene–Pleistocene stack of 57 globally distributed benthic ∂18O records. Paleoceanography 20, PA1003. doi:10.1029/2004PA001071.

Lisiecki, L.E., Raymo, M.E., 2007. Plio-Pleistocene climate evolution: trends and transition in glacial cycle dynamics. Quaternary Science Reviews 26, 56–69.

Lisiecki, L.E., Raymo, M.E., Curry, W.B., 2008. Atlantic overturning responses to late Pleistocene climate forcings. Nature 456, 85–88.

Liu, Z., Herbert, T.D., 2004. High-latitude influence on the eastern equatorial Pacific climate in the early Pleistocene epoch. Nature 427, 720–723.

Locarnini, R.A., Mishonov, A.V., Antonov, J.I., Boyer, T.P., Garcia, H.E., 2006. World Ocean Atlas 2005, Volume 1. Temperature, Edited, p. 182, NOAA Atlas NESDIS 61, U.S. Government Printing Office, Washington, D.C.

Lunt, D.J., Foster, G.L., Haywood, A.M., Stone, E.J., 2008. Late Pliocene Greenland glaciation controlled by a decline in atmospheric CO_2 levels. Nature 454, 1102–1105.

Manabe, S., Broccoli, A.J., 1985. The influence of continental ice sheets on the climate of an ice age. Journal of Geophysical Research 90, 2167–2190.

Marlowe, I.T., Green, J.C., Neal, A.C., Brassell, S.C., Eglinton, G., 1984. Long chain alkenones in the Prymnesiophyceae. Distribution of alkenones and other lipids and their taxonomic significance. British Phycological Journal 19, 203–216.

Martinez-Garcia, A., Rosell- Mele, A., Geibert, W., Gersonde, R., Masque, P., Gaspari, V., Barbante, C., 2009. Links between iron supply, marine productivity, sea surface temperature, and CO_2 over the last 1.1 Ma. Paleoceanography 24, PA1207. doi:10.1029/2008PA001657.

McClymont, E.L., Rosell-Mele, A., Haug, G., Lloyd, J.M., 2008. Expansion of subarctic water masses in the North Atlantic and Pacific oceans and implications for mid-Pleistocene ice sheet growth. Paleoceanography 23, PA4214. doi:10.1029/2008PA001622.

Medina-Elizalde, M., Lea, D.W., 2005. The mid-Pleistocene transition in the tropical Pacific. Science 310 (5750), 1009–1012.

Medina-Elizalde, M., Lea, D., 2010. Late Pliocene equatorial Pacific. Paleoceanography 25, PA2208. doi:10.1029/2009PA001780.

Mudelsee, M., Raymo, M.E., 2005. Slow dynamics of the northern hemisphere glaciation. Paleoceanography 20, PA4022. doi:10.1029/2005PA001153.

Müller, P.J., Kirst, G., Ruhland, G., von Storch, I., Rosell-Melé, A., 1998. Calibration of the alkenone paleotemperature index $U_{37}^{k'}$ on core-tops from the eastern South Atlantic and the global ocean (60°N–60°S). Geochemica Cosmochimica Acta 62 (10), 1757–1772.

Naish, T., Powell, R., Levy, R., Wilson, G., Scherer, R., Talarico, F., Krissek, L., Niessen, F., Pompilio, M., Wilson, T., Carter, L., DeConto, R., Huybers, P., McKay, R., Pollard, D., Ross, J., Winter, D., Barrett, P., Browne, G., Cody, R., Cowan, E., Crampton, J., Dunbar, G., Dunbar, N., Florindo, F., Gebhardt, C., Graham, I., Hannah, M., Hansaraj, D., Harwood, D., Helling, D., Henrys, S., Hinnov, L., Kuhn, G., Kyle, P., Laufer, A., Maffioli, P., Magens, D., Mandernack, K., McIntosh, W., Millan, C., Morin, R., Ohneiser, C., Paulsen, T., Persico, D., Raine, I., Reed, J., Riesselman, C., Sagnotti, L., Schmitt, D., Sjunneskog, C., Strong, P., Taviani, M., Vogel, S., Wilch, T., Williams, T., 2009. Obliquity-paced Pliocene West Antarctic ice sheet oscillations. Nature 458 (7236), 322–U384.

Oppo, D.W., Fairbanks, R.G., 1987. Variability in the depp and intermediate water circulation of the Atlantic Ocean during the past 25,000 years: northern hemisphere modulation of the Southern Ocean. Earth and Planetary Science Letters 86, 1–15.

Pagani, M., Liu, Z., LaRiviere, J.P., Ravelo, A.C., 2009. High Earth-system climate sensitivity determined from Pliocene carbon dioxide concentrations. Nature Geoscience 3, 27–30.

Paillard, D., 1998. The timing of Pleistocene glaciations from a simple multiple-state climate model. Nature 391, 378–381.

Pisias, N.G., Moore, T.C., 1981. The evolution of the Pleistocene climate: a time series approach. Earth and Planetary Science Letters 52, 450–458.

Pollard, D., DeConto, R.M., 2009. Modelling West Antarctic ice sheet growth and collapse through the past five million years. Nature 458 (7236), 329–U389.

Prahl, F.G., Wakeham, S.G., 1987. Calibration of unsaturation patterns in long-chain ketone compositions for palaeotemperature assessment. Nature 330, 367–369.

Prahl, F.G., Muehlhausen, L.A., Zahnle, D.L., 1988. Further evaluation of long-chain alkenones as indicators of paleoceanographic conditions. Geochemica Cosmochimica Acta 52, 2303–2310.

Ravelo, A.C., Andreasen, D.H., Lyle, M., Lyle, A.O., Wara, M.W., 2004. Regional climate shifts caused by gradual global cooling in the Pliocene epoch. Nature 429, 263–267.

Ravelo, A.C., Billiups, K., Dekens, P.S., Herbert, T.D., Lawrence, K.T., 2007. Onto the ice ages: proxy evidence for the onset of northern hemisphere glaciation. In: Williams, M., Haywood, A.M.J.G. (Eds.), Deep Time Perspectives on Climate Change. The Micropalaeontological Society, pp. 563–574.

Raymo, M.E., 1994. The initiation of northern hemisphere glaciation. Annual Review of Earth and Planetary Sciences 22, 353–383.

Raymo, M.E., 1997. The timing of major climate terminations. Paleoceanography 12, 577–585.

Raymo, M.E., Ruddiman, W.F., Clement, B.M., 1986. Pliocene/Pleistocene paleoceanography of the North Atlantic at DSDP 609. Initial Reports of the Deep Sea Drilling Project 94, 895–901.

Raymo, M.E., Ruddiman, W.F., Backman, J., Clement, B.M., Martinson, D.G., 1989. Late Pliocene variation in northern hemisphere ice sheets and North Atlantic Deep Water circulation. Paleoceanography 4, 413–446.

Raymo, M.E., Hodell, D., Jansen, E., 1992. Response of Deep Ocean Circulation to the initiation of Northern Hemisphere Glaciation (3-2 Ma). Paleoceanography 7, 645–672.

Raymo, M.E., Grant, B., Horowitz, M., Rau, G.H., 1996. Mid-Pliocene warmth: stronger greenhouse and stronger conveyor. Marine Micropaleontology 27, 313–326.

Raymo, M.E., Oppo, D.W., Curry, W.B., 1997. The mid-Pleistocene climate transition: a deep sea carbon perspective. Paleoceanography 12 (4), 546–559.

Raymo, M.E., Lisiecki, L.E., Nisancioglu, K., 2006. Plio-Pleistocene ice volume, Antarctic climate, and the global ∂18O record. Science 313, 492–495.

Rial, J.A., 2004. Abrupt climate change: chaos and order at orbital and millennial scales. Global and Planetary Change 41, 95–109.

Robinson, M.M., Dowsett, H.J., Dwyer, G.S., Lawrence, K.T., 2008. Re-evaluation of mid-Pliocene North Atlantic sea-surface temperature. Paleoceanography 23, PA3213. doi:10.1029/2008PA001608.

Roy, M., Clark, P.U., Barendregt, R.W., Glassman, J.R., Enkin, R.J., Baker, J., 2004. Glacial stratigraphy and paleomagnetism of late Cenozoic deposits of the north-central US. Geological Society of America Bulletin 116, 30–41.

Ruddiman, W.F., McIntyre, A., 1984. Ice-age thermal response and climatic role of the surface North Atlantic Ocean. Geological Society of America Bulletin 95, 381–396.

Ruddiman, W.F., Raymo, M.E., Martinson, D.G., Clement, B.M., Backman, J., 1989. Pleistocene evolution: northern hemisphere ice sheets and North Atlantic Ocean. Paleoceanography 4, 353–412.

Seidov, D., Barron, E.J., Haupt, B.J., 2001. Meltwater and the global ocean conveyor: northern versus southern connections. Global and Planetary Change 30, 257–270.

Seki, O., Foster, G.L., Schmidt, D.N., Mackensen, A., Kawamura, K., Pancost, R.D., 2010. Alkenone and boron-based Pliocene PCO_2 records. Earth and Planetary Science Letters 292, 201–211.

Shackleton, N.J., 2000. The 100,000-year ice-age cycle identified and found to lag temperature, carbon dioxide, and orbital eccentricity. Science 289, 1897–1902.

Shackleton, N.J., Opdyke, N.D., 1976. Oxygen-isotope and paleomagetic stratigraphy of Pacific core V28-239: late Pliocene to latest Pleistocene. Geological Society America Memoir 145, 449–464.

Shackleton, N.J., Backman, J., Zimmerman, H., Kent, D.V., Hall, M.A., Roberts, D., Schnitker, D., Baldauf, J.G., Desprairies, A., Homrighausen, R., Huddlestun, P., Keene, J.B., Kaltenbach, A.J., Krumsick, K.A.O., Morton, A.C., Murray, J.W., Westberg-Smith, J., 1984. Oxygen isotope calibration on the onset of ice-rafting and history of glaciation in the North Atlantic region. Nature 307, 620–623.
Skinner, L.C., Shackleton, N., 2006. Deconstructing Terminations I and II: revisiting the glacioeustatic paradigm based on deep-water temperature estimates. Quaternary Science Reviews 25, 3312–3321.
Sosdian, S., Rosenthal, Y., 2009. Deep-sea temperature and ice volume changes across the Pliocene–Pleistocene climate transition. Science 325, 306–310.
St. John, K.E.K., Krissek, L.A., 2002. The late Miocene to Pleistocene ice-rafting history of southeast Greenland. Boreas 31, 28–35.
Steph, S., Tiedemann, R., Prange, M., Groeneveld, J., Schulz, M., Timmerman, A., Nurnberg, D., Ruhlemann, C., Saukel, C., Haug, G., 2010. Early Pliocene increase in thermohaline overturning: a precondition for the development of the modern equatorial Pacific cold tongue. Paleoceanography 25, PA2202. doi:10.1029/2008PA001645.
Stocker, T.F., Wright, D.G., Broecker, W.S., 1992. The influence of high-latitude surface forcing on the global thermohaline circulation. Paleoceanography 7, 529–541.
Stott, L.D., Timmerman, A., Thunell, R., 2007. Southern hemisphere and deep-sea warming led deglacial atmospheric CO_2 rise and tropical warming. Science 318, 435–438.
Toggweiler, J.R., Russell, J.L., Carson, S.R., 2006. Midlatitude westerlies, atmospheric CO_2, and climate change during the ice ages. Paleoceanography 31, PA2005. doi:10.1029/2005PA001154.
Tripati, A.K., Robert, C.D., Eagle, R.A., 2009. Coupling of CO_2 and ice sheet stability over major climate transitions of the last 20 million years. Science 326, 1394–1397.
Van Der Burgh, J., Visscher, H., Dilcher, D.L., Kurschner, W.M., 1993. Paleoatmospheric signatures in Neogene fossil leaves. Science 260, 1788–1790.
Venz, K.A., Hodell, D.A., 2002. New evidence for changes in Plio-Pleistocene deep water circulation from Southern Ocean ODP Leg 177 Site 1090. Palaeogeography, Palaeoclimatology, Palaeoecology 182 (3–4), 197–220.
Wara, M.W., Ravelo, A.C., Delaney, M.L., 2005. Permanent El Nino-like conditions during the Pliocene warm period. Science 309, 758–761.
Wright, A.K., Flower, B.P., 2002. Surface and deep ocean circulation in the subpolar North Atlantic during the mid-Pleistocene revolution. Paleoceanography 17 (4). doi:10.1029/2002PA000782.